Macromolecules **2007,** *40,* 4088−4091

Notes

Interaction of Solid Surfaces Across Binary Mixtures of Polymer Melts

Rüdiger Stark, Michael Kappl, and Hans-Jürgen Butt*

Max-Planck-Institute for Polymer Research, Ackermannweg 10, 55128 Mainz, Germany

Received January 4, 2007
Revised Manuscript Received March 20, 2007

Polymers in contact with a inorganic solid surface have been studied intensively because of the relevance in applications such as adhesion, the fabrication of composite materials, and for fundamental reasons. When dealing with polydisperse polymers or mixtures of polymers of different molecular weight, one fundamental question is whether short or long chains are enriched or depleted at the interface. The enthalpy of adsorption should not have an influence because segments of short and long chains bind equally well to the interface. Therefore, entropic effects should dominate, assuming that the end groups do not bind specifically. Polymer chains at a solid interface suffer from a loss of configurational entropy and they avoid the interface. This effect is stronger for long chains, which should lead to a depletion of long chains and an enrichment of short chains.[1−5] This prediction was confirmed for example by measuring the surface tension of polymers of different molecular weights. The surface tension increases with increasing molecular weight.[6−11] Direct evidence of the enrichment of short chains at a free polymer surface was obtained by neutron reflectivity measurements of blends of hydrated and deuterated polystyrene near the air surface[12,13] by surface-enhanced Raman spectroscopy[14] and by secondary ion mass spectrometry.[13]

In this paper, we describe results obtained with melts of unlabeled poly(dimethyl siloxane) (PDMS). The melts contained a bimodal distribution of short and long chains. A previous study[15] showed that the presence of short or long PDMS chains at a silicon oxide surface can be discriminated by surface force measurements with the atomic force microscope (AFM). In a melt of short chains ($M_w \leq 6$ kDa), attractive forces were measured. In a melt of long chains ($M_w \geq 9$ kDa), only repulsive forces were present. Thus a measurement of surface forces should allow to determine if short or long chains dominate the force.

PDMS was synthesized from the trimer hexamethylcyclotrisiloxane by an anionic ring-opening polymerization. Ten percent of the monomer was dissolved in freshly distilled cyclohexane and *sec*-butyl-lithium was added as a starter. After 10 h, the rest of the monomer was added in a THF−cyclohexane mixture (60:40). The product was purified with a fractionator. PDMS of the following molecular weights M_w and polydispersities M_w/M_n (determined by gel permeation chromatography) were synthesized and studied: 4.2 kDa and 1.42, 5.9 kDa and 1.38, 17 kDa and 1.05, 18 and 1.04, 19 kDa and 1.05, 20 kDa and 1.07. To keep the polymers water free, all samples were stored under vacuum and on molecular sieves. In addition, a high-molecular-weight OH-terminated PDMS was synthesized by quenching the reaction with MeOH ($M_w = 20$ kDa, $M_w/M_n = 1.07$). Mixtures were made by adding the two volume fractions in a reaction tube and mixing with a pipet for 1−2 min.

As a solid surface, we used naturally oxidized silicon wafers ({100}, Si-mat Silicon Materials, Landsberg, Germany). PDMS spread on the wafer, and the contact angle was zero. For a force measurement, the silicon wafer was mounted onto the piezoelectric AFM scanner (Nanoscope 3 multimode, Veeco Instruments, Santa Barbara, CA). Then the AFM head with the liquid cell without an O-ring and the cantilever were mounted, and the liquid cell was filled with polymer melt. The system was allowed to equilibrate for 10 h. The temperature of the cell was 28 °C. During a force measurement, the sample was periodically moved up and down at constant driving velocity of 10−50 nm/s while the cantilever deflection was measured with the optical lever technique. The result of such a measurement is a plot of cantilever deflection vs position of the piezoelectric translator. From this, a force-vs-distance curve, briefly called “force curve”, was calculated by multiplying the cantilever deflection with the spring constant to obtain the force and subtracting the cantilever deflection from the position of the piezo to obtain the distance. Apparent contact was derived from the linear contact part of force curves (details in ref 16). We call it “apparent contact” rather than zero distance because it cannot be excluded that a thin, incompressible layer of polymer is still present between tip and sample. Figures typically show 10−30 force curves plotted together to allow for a visual averaging and to be able to estimate the noise level. V-shaped cantilevers with silicon nitride tips (length 120 μm, width of each arm 18 μm, thickness 0.6 μm, Veeco Instruments, Santa Barbara, CA) were used. They were cleaned in a plasma cleaner for 5 min at 30 W in an argon atmosphere of 0.1−1 mbar before each measurement. The radius of the tip curvature was determined with a scanning electron microscope (SEM, LEO 1530 Gemini, Oberkochen, Germany). Radii of curvature were $R = 15−110$ nm with an error of 20% and at least 5 nm. Cantilever spring constants were individually determined by the thermal noise method[17,18] with a molecular force probe (MFP-1D, Asylum Research, Santa Barbara, CA). They were 0.2−0.6 N/m. For each experiment, a new cantilever was used to avoid contamination with polymer of the previous experiment.

Force curves recorded in long-chain PDMS ($M_w = 17$, 19, 18, and 20 kDa) were repulsive (Figure 1A).[19] When plotting force curves in a double-logarithmic scale (Figure 1A inset), two regimes can be distinguished. Each regime is characterized by a straight line. In each regime, the force F can be described by a power law $F \propto 1/D^n$, where D is the distance. For close distances ($D \leq 1$ nm), the force decays with an exponent $n = 0.4$. At larger distances, the exponent increases to $n = 1.5$. For

---

* Corresponding author. E-mail: butt@mpip-mainz.mpg.de. Telephone: 0049-6131-379 111. Fax: 0049-6131-379 310.

10.1021/ma070024r CCC: $37.00

mixtures with a volume ratio of short chains of $\varphi = 0.1$ also a repulsive force was observed on approach (Figure 1B), which again in the log−log plot (Figure 1B inset) revealed two regimes. For distances below 2.5 nm, it could be described by a power law with $n = 0.8$. For larger distances, a power law with $n = 1.5$ dominated.

Before interpreting the results, it is instructive to recall which forces are expected. Theory[20,21] and MC simulations[22] agree that, in a melt in perfect thermodynamic equilibrium, no force at all should be present. Negligible forces were indeed observed in polyisoprene by AFM experiments.[23] If the polymer chains are fixed to the interacting surface on the time scale of an approach, this should lead to repulsion. Thus we attribute repulsive forces to the formation of an immobilized layer.[20,24] Immobilized layers in polymer melts were also observed in experiments with the surface forces apparatus.[25−34] Polymer molecules in direct contact with the solid interface were not able to equilibrate with the bulk polymer on the time scale of taking one force curve. In AFM experiments, this time scale is of the order of 0.1 s. Upon approach of the tip, the adsorbed or “pinned” chains are compressed, which leads to a steric repulsive force (for a detailed discussion see ref 23).

For distances larger than 1−2 nm, the repulsive force could indeed be fitted with the simple model for a polymer brush in good solvent proposed by de Gennes[35] and refined by Milner, Witten, and Cates.[36] If the thermal movement of a polymer chain at a surface is limited by the approach of another surface, then the entropy of the individual polymer chain decreases. The resulting force between a tip with a spherical end and a planar surface is[35]

$$\frac{F}{R} = \frac{16\pi}{35} k_B T L_0 \Gamma^{3/2}\left[7\left(\frac{D}{2L_0}\right)^{-5/4} + 5\left(\frac{D}{2L_0}\right)^{7/4} - 12\right] \quad (1)$$

for $D < 2L_0$. Here, k_B and T are the Boltzmann’s constant and the temperature. L_0 is the thickness of the brush, and Γ is the grafting density. Good fits were obtained with $L_0 = 7$ nm and $\Gamma = 1.9 \times 10^{16}$ m^{-2} for pure long chains, and $L_0 = 9$ nm and $\Gamma = 1.1 \times 10^{16}$ m^{-2} for $\varphi = 0.1$ (10 vol % short-chain PDMS).

When increasing the amount of short-chain PDMS to $\varphi = 0.2$, the force became attractive (Figure 1C). The attraction increased up to $\varphi = 0.5$ and, except for one experiment, was constant up to pure short-chain PDMS (Figure 1D,E). To quantify this change from repulsion to attraction and the increase in attraction, we calculated the “approaching energy” per unit area (Figure 2A). This approaching energy is the work done to bring the tip into apparent contact with the sample surface. It corresponds to the area between the force curve and the *x*-axis (distance). For $\varphi \leq 0.1$, the approaching energy is positive. For $\varphi = 0.2$ and higher, it becomes negative because the force is attractive. We would like to point out that the error in the approaching energy is of the order of a factor of 2. This error was estimated from results obtained with similar polymer mixtures.

We do not know why strong attractive forces occur at all. A van der Waals attraction calculated with $F/R = A/(6D^2)$ and a Hamaker constant for silicon oxide interacting with silicon nitride in PDMS[19] of $A = 8.8 \times 10^{-21}$ J leads to forces that are 10 times lower than what was observed. Electrostatic attraction caused by contact charging during the separation of the tip from the substrate is not likely because the attraction is constant irrespective of a waiting period between two force curves. In any case, the presence of attractive forces indicates that no immobilized layer is formed at the surfaces.

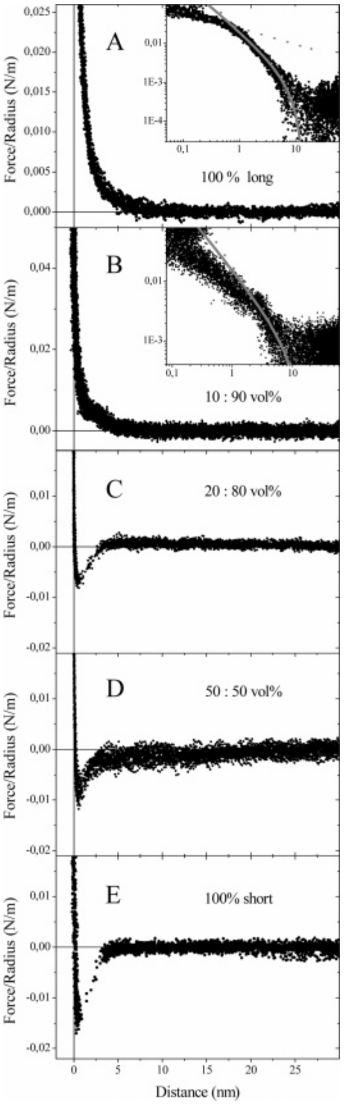

Figure 1. Approaching force-vs-distance curves measured on a silicon wafer in different mixtures of short and long-chain PDMS. (A) Pure long-chain PDMS ($M_w = 18$ kDa, $R = 110$ nm). Inset: Same force curve on a log−log scale. It includes a fit with the model of de Gennes eq 1 as a gray continuous line ($L_0 = 7$ nm, $\Gamma = 1.9 \times 10^{16}$ m^{-2}). The dashed lines indicate the two regimes dominated by different power laws. (B) Mixture of 5.9 kDa and 19 kDa PDMS with 10 vol % short chains ($\varphi = 0.1$, $R = 75$ nm). Inset: Force curve was fitted with eq 1 ($L_0 = 9$ nm, $\Gamma = 1.1 \times 10^{16}$ m^{-2}, continuous gray line). (C) Mixtures with $\varphi = 0.2$ ($R = 75$ nm). (D) Mixture with $\varphi = 0.5$ ($R = 30$ nm). (E) Pure short-chain PDMS ($M_w = 4.2$ kDa, $R = 62$ nm).

The change from repulsion to attraction occurred at a low volume fraction of $\varphi = 0.1−0.2$. Even the presence of 10−20% short-chain polymer destroys the repulsive force. Two reasons are possible: (1) Short chains are enriched at the surface. (2) Even a small amount of short chains could hinder the formation of an immobilized layer. To estimate the degree of surface segregation, we used an equation derived by the numerical self-consistent field model of Scheutjens and Fleer and an analytical approximation.[4,5] For bimodal weight distributions, the entropically driven surface excess of the short-chain polymer of molar mass M_s in a mixture with an average molar mass $\bar{M}$ (both weight molar masses) and a bulk volume fraction φ is

$$\Gamma = 0.195 \cdot \varphi\left(1 - \frac{M_s}{\bar{M}}\right) \quad (2)$$

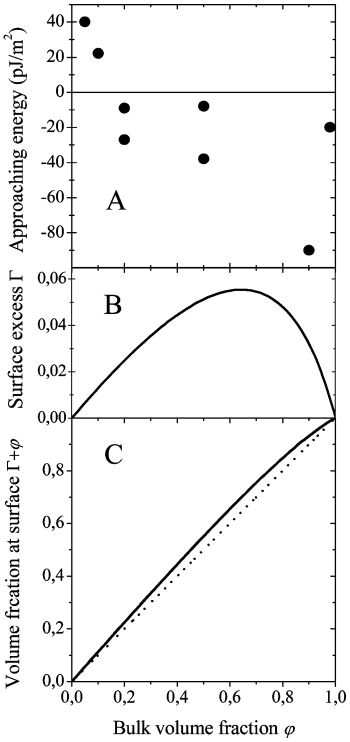

Figure 2. (A) "Approaching energy" per unit area vs bulk volume fraction φ of short chains. The approaching energy is the work required to bring the tip into apparent contact with the sample surface. Positive energies correspond to repulsive forces, negative values to attractive force. (B) Surface excess of short chains Γ at the surface as calculated with eq 2. (C) Local volume fraction of short chains at the surface $\varphi + \Gamma$ as calculated with eq 2.

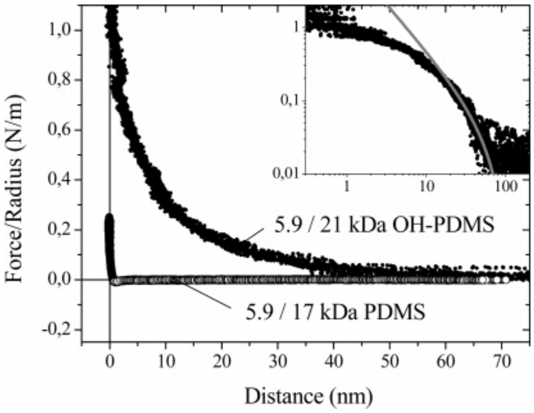

Figure 3. Approaching force curves showing 50:50 (vol %) mixtures of 5.9/17 kDa PDMS both methyl terminated and 5.9 kDa methyl-terminated with 21 kDa hydroxyl-terminated PDMS. Inset: Approaching force-vs-distance curve for 5.9/21 kDa mixture in double-logarithmic scale. The gray line is a fit with eq 1 using $L_0 = 55$ nm and $\Gamma = 4.9 \times 10^{16}$ m^{-2}.

For mixtures of 5.9 and 19 kDa PDMS, the local volume fraction at the surface, $\Gamma + \varphi$, is at most 5.6% higher than the bulk volume fraction (Figure 2B,C). Thus, surface segregation alone cannot explain the change from repulsion to attraction at $\varphi = 0.1-0.2$, and we believe that the presence of short chains hinders the formation of an immobilized layer.

For PDMS with methyl end groups, the enrichment of low-molecular-weight polymer at the surface is dominated by entropy. By attaching a hydroxyl group to one end of the polymer chain, enthalpic contributions become relevant.[3,37] To verify this, we measured forces in melts containing hydroxyl-terminated PDMS. The terminal hydroxyl groups bind to the oxidized silicon wafer surface and the oxidized silicon nitride tip surface.[38] When mixing hydroxyl-terminated PDMS with low-molar-mass methyl-terminated PDMS, a repulsion is observed for a 50:50 mixture (Figure 3). We interpret the repulsive force as being due to the formation of a brushlike structure of PDMS−OH at the surface. A brush formed by polymer chains with an adsorbing end leads to a steric repulsion.[35,36,39−43] To accommodate many hydroxyl groups on the surface, the adsorbed chains will deform from the random coil to a more stretched configuration, which leads to a brushlike structure. When fitting the force with eq 1, typical brush thicknesses of $L_0 = 50$ nm and grafting densities of $\Gamma = 5 \times 10^{16}$ m^{-2} were found. Considering that the contour length of the PDMS−OH is 80 nm ($M_w = 21$ kDa) and considering the mean distance between grafting sites at $\Gamma = 5 \times 10^{16}$ m^{-2} is 4 nm, this confirms the strong adsorption of the hydroxyl groups to the silicon oxide surface and the formation of a brush.

Acknowledgment. We thank J. Thiel and T. Wagner for synthesizing the polymers.

References and Notes

(1) Hariharan, A.; Kumar, S. K.; Russell, T. P. *Macromolecules* **1990**, *23*, 3584−3592.
(2) Kumar, S. K.; Vocatello, M.; Yoon, D. Y. *Macromolecules* **1990**, *23*, 2189−2197.
(3) Manghi, M.; Aubouy, M. *Adv. Colloid Interface Sci.* **2001**, *94*, 21−31.
(4) Van der Guecht, J.; Besseling, N. A. M.; Fleer, G. J. *Macomolecules* **2002**, *35*, 6732−6738.
(5) Dolinnyi, A. I. *Colloid J.* **2006**, *68*, 37−45.
(6) LeGrand, D. G.; Gaines, G. L. *J. Colloid Interface Sci.* **1973**, *42*, 181−184.
(7) Bhatia, Q. S.; Pan, D. H.; Koberstein, J. T. *Macromolecules* **1988**, *21*, 2166−2175.
(8) Anastasiadis, S. H.; Gancarz, I.; Koberstein, J. T. *Macromolecules* **1988**, *21*, 2980−2987.
(9) Jalbert, C.; Koberstein, J. T.; Yilgor, I.; Gallagher, P.; Krukonis, V. *Macromolecules* **1993**, *26*, 3069−3074.
(10) Hong, P. P.; Boerio, F. J.; Smith, S. D. *Macomolecules* **1994**, *27*, 596−605.
(11) Sauer, B. B.; Dee, G. T. *J. Colloid Interface Sci.* **1994**, *162*, 25−35.
(12) Hariharan, A.; Kumar, S. K.; Russell, T. P. *J. Chem. Phys.* **1993**, *98*, 4163−4173.
(13) Tanaka, K.; Kajiyama, T.; Takahara, A.; Tasaki, S. *Macomolecules* **2002**, *35*, 4702−4706.
(14) Hong, P. P.; Boerio, F. J.; Smith, S. D. *Macromolecules* **1993**, *26*, 1460−1464.
(15) Sun, G.; Stark, R.; Kappl, M.; Leermakers, F. A. M.; Butt, H.-J. *Compos. Interfaces* **2005**, *12*, 805−815.
(16) Butt, H.-J.; Cappella, B.; Kappl, M. *Surf. Sci. Rep.* **2005**, *59*, 1−152.
(17) Hutter, J. L.; Bechhoefer, J. *Rev. Sci. Instrum.* **1993**, *64*, 1868−1873.
(18) Butt, H.-J.; Jaschke, M. *Nanotechnology* **1995**, *6*, 1−7.
(19) Sun, G.; Kappl, M.; Pakula, T.; Kremer, K.; Butt, H.-J. *Langmuir* **2004**, *20*, 8030−8034.
(20) de Gennes, P. G. *C.R. Acad. Sci. Paris* **1987**, *305*, 1181−1184.
(21) Ausserré, D. *J. Phys. (Paris)* **1989**, *50*, 3021−3042.
(22) ten Brinke, G.; Ausserre, D.; Hadziioannou, G. *J. Chem. Phys.* **1988**, *89*, 4374−4380.
(23) Stark, R.; Bonaccurso, E.; Kappl, M.; Butt, H. J. *Polymer* **2006**, *47*, 7259−7270.
(24) Leermakers, F. A. M.; Butt, H.-J. *Phys. Rev. E* **2005**, *72*, 021807.
(25) Horn, R. G.; Israelachvili, J. N. *Macromolecules* **1988**, *21*, 2836−2841.
(26) Hirz, S.; Subbotin, A.; Frank, C.; Hadziioannou, G. *Macromolecules* **1996**, *29*, 3970−3974.
(27) Montfort, J. P.; Hadziioannou, G. *J. Chem. Phys.* **1988**, *88*, 7187−7196.
(28) van Alsten, J.; Granick, S. *Macromolecules* **1990**, *23*, 4856−4862.
(29) Luengo, G.; Schmitt, F. J.; Hill, R.; Israelachvili, J. *Macromolecules* **1997**, *30*, 2482−2494.
(30) Granick, S.; Hu, H. W. *Langmuir* **1994**, *10*, 3857−3866.
(31) Yu, C.; Evmenenko, G.; Kmetko, J.; Dutta, P. *Langmuir* **2003**, *19*, 9558−9561.
(32) Evmenenko, G.; Mo, H.; Kewalramani, S.; Dutta, P. *Polymer* **2006**, *47*, 878−882.

(33) Litvinov, V. M.; Barthel, H.; Weis, J. *Macromolecules* **2002**, *35*, 4356−4364.

(34) Hartmann, L.; Kremer, F.; Pouret, P.; Léger, L. *J. Chem. Phys.* **2003**, *118*, 6052−6058.

(35) de Gennes, P. G. *Adv. Colloid Interface Sci.* **1987**, *27*, 189−209.

(36) Milner, S. T.; Witten, T. A.; Cates, M. E. *Macromolecules* **1988**, *21*, 2610−2619.

(37) Jalbert, C.; Koberstein, J. T.; Hariharan, A.; Kumar, S. K. *Macomolecules* **1997**, *30*, 4481.

(38) Tsige, M.; Soddemann, T.; Rempe, S. B.; Grest, G. S.; Kress, J. D.; Robbins, M. O.; Sides, S. W.; Stevens, M. J.; Webb, E. *J. Chem. Phys.* **2003**, *118*, 5132−5142.

(39) Ash, S. G.; Findenegg, G. H. *Trans. Faraday Soc.* **1971**, *67*, 2122.

(40) Dolan, A. K.; Edwards, S. F. *Proc. R. Soc. London, Ser. A* **1974**, *337*, 509−516.

(41) Patel, S.; Tirrell, M.; Hadziioannou, G. *Colloids Surf.* **1988**, *31*, 157−179.

(42) Taunton, H. J.; Toprakcioglu, C.; Fetters, L. J.; Klein, J. *Macromolecules* **1990**, *23*, 571−580.

(43) Klein, J.; Perahia, D.; Warburg, S. *Nature* **1991**, *352*, 143−145.

MA070024R